Evaluation of Structural Robustness against Column Loss: Methodology and Application to RC Frame Buildings

Yihai Bao, A.M.ASCE[1], Joseph A. Main, M.ASCE[2], and Sam-Young Noh[3]

Abstract: A computational methodology is presented for evaluating structural robustness against column loss. The methodology is illustrated through application to reinforced concrete (RC) frame buildings, using a reduced-order modeling approach for three-dimensional RC framing systems that includes the floor slabs. Comparisons with high-fidelity finite-element model results are presented to verify the approach. Pushdown analyses of prototype buildings under column loss scenarios are performed using the reduced-order modeling approach, and an energy-based procedure is employed to account for the dynamic effects associated with sudden column loss. Results obtained using the energy-based approach are found to be in good agreement with results from direct dynamic analysis of sudden column loss. A metric for structural robustness is proposed, calculated by normalizing the ultimate capacities of the structural system under sudden column loss by the applicable service-level gravity loading and by evaluating the minimum value of this normalized ultimate capacity over all column removal scenarios. The procedure is applied to two prototype 10-story RC buildings, one employing intermediate moment frames (IMFs) and the other employing special moment frames (SMFs). The SMF building, with its more stringent seismic design and detailing, is found to have greater robustness.

Keywords: Analysis and computation; Buildings; Column loss; Disproportionate collapse; Finite-element method; Nonlinear analysis; Reinforced concrete structures.

---

[1] IPA Researcher, National Institute of Standards and Technology, Gaithersburg, MD 20899, yihai.bao@nist.gov, and Assistant Project Scientist, University of California-Davis, Davis, CA 961155, ybao@ucdavis.edu
[2] Research Structural Engineer, National Institute of Standards and Technology, Gaithersburg, MD 20899, joseph.main@nist.gov
[3] Associate Professor, Dept. of Architectural Eng., Hanyang University, Ansan, 15588, Korea, noh@hanyang.ac.kr

NOTICE: This is the authors' version of an article that was accepted for publication in the *Journal of Structural Engineering*. A definitive version is available at https://doi.org/10.1061/(ASCE)ST.1943-541X.0001795.

Introduction

In the context of structural design, the term *robustness* has been used to indicate the ability of a structure to resist damage under abnormal loads. Two prominent definitions of structural robustness, from the U.S. General Services Administration (GSA 2003) and the European Committee for Standardization (CEN 2006), are listed in Table 1. Starossek and Haberland (2010) proposed that these definitions, as well as others they reviewed, could be summarized by defining structural robustness as "insensitivity of a structure to initial damage," noting that "a structure is robust if an initial damage does not lead to disproportionate collapse." A number of factors contribute to the robustness of a structure, including redundancy, ductility supply, and energy absorption capacity. However, as discussed by Izzuddin et al. (2008), none of these factors alone is adequate to serve as a measure of structural robustness, because they cannot, in isolation, ensure the robustness of a structural system.

Recognizing the value of a quantitative, rather than purely qualitative, characterization, a number of researchers have proposed metrics for structural robustness. In evaluating these proposed metrics, it is helpful to consider the requirements proposed by Starossek and Haberland (2009), that a measure of robustness should be expressive (allowing for a clear differentiation between robust and non-robust structures), objective, simple, and calculable. Baker et al. (2008) proposed risk-based index of robustness as the ratio between the direct risk and the total risk associated with potentially damaging events, where the total risk includes indirect consequences. Calculability is a challenge with such risk-based approaches, because the relevant event probabilities are generally not well characterized in a practical design context. A stiffness-based robustness measure was proposed by Starossek and Haberland (2009), who noted that this metric was readily calculable but was not sufficiently expressive, because it did not correlate well with

the reduction in load capacity after the loss of structural elements. Nafday (2011) also outlined the possibility of a stiffness-based metric for robustness, but noted that future work is needed to develop such a metric. Starossek and Haberland (2009) proposed an energy-based robustness measure that quantifies the potential for collapse progression, but noted that this measure is expressive only for relatively simple chain-like structures.

A number of researchers have also proposed damage-based measures of structural robustness. Starossek and Haberland (2009) proposed two alternative damage-based measures of robustness, which involve comparing the maximum extent of damage to the initial damage. However, as Starossek and Haberland (2009) note, calculability can be a significant challenge for such an approach, as determination of the maximum extent of damage requires dynamic analysis of collapse progression, in which separation and impact events can play an important role. A provocative word of caution from Powell (2009) may be in order with regard to the difficulties of such a direct simulation of structural collapse progression: "Any engineer who claims the ability to do such an accurate simulation is at least disingenuous, and possibly delusional." A damage-based robustness metric was proposed by Cranford et al. (2012) in evaluating the robustness of spider webs, in which structural robustness was defined as the undamaged fraction of the web after failure. Fascetti et al. (2015) proposed an analysis procedure that involves determination of the most critical sequence for successive removal of multiple columns, defining a robustness index as the minimum fraction of columns that must be removed to cause failure. Formisano et al. (2015) derived a damage-based deterministic approach from the risk-based approach of Baker et al. (2008), defining a robustness index in terms of the ratio of the direct damage in an event to the total damage, including indirect damage.

While challenges remain for many of the proposed robustness metrics outlined above, consensus has been growing among a number of researchers about the appropriateness of a robustness metric based on the ultimate capacity of a damaged structural system (Izzuddin et al. 2008, Lu et al. 2010, Khandelwal and El-Tawil 2011, Raebel 2011, Xu and Ellingwood 2012, Main 2014). In this capacity-based approach, the ultimate capacity of a structure under column loss scenarios is evaluated using nonlinear static pushdown analysis and/or incremental dynamic analysis (e.g., Khandelwal and El-Tawil 2011), in which successive dynamic analyses of sudden column loss are performed under increasing levels of gravity loading. In conjunction with static pushdown analyses, energy-based analysis has been used to account for the dynamic effects associated with sudden column loss (Powell 2003, Izzuddin et al. 2008; Xu and Ellingwood 2012; Main 2014). Different normalizations have been proposed for the ultimate capacities of damaged structural systems, with Khandelwal and El-Tawil (2011) proposing an "overload factor" obtained by dividing the failure load by the nominal gravity loads, and Raebel (2011) defining a robustness measure by normalizing changes in the system capacity relative to the capacity of a base system.

In this study, a methodology for evaluation of structural robustness is proposed that builds on and integrates various aspects of the capacity-based procedures outlined above. In considering the appropriate definition of a robustness index, it is helpful to consider a more precise definition of structural robustness proposed by Starossek and Haberland (2010): "a structure is robust if an initial damage as determined from the hazard scenarios does not lead to an extent of collapse or other damage that violates the performance objectives." In this study, the selected performance objective is to sustain the applicable gravity loading on the floor system. By normalizing the ultimate capacity of the system by the applicable gravity loading, the performance objective is

met provided that the normalized capacity remains greater than unity under all initial damage scenarios. The robustness index is defined as the minimum value of the normalized ultimate capacity over all damage scenarios. The proposed capacity-based robustness metric is more readily calculable than the damage-based approaches that require calculating the extent of damage, because the analysis can be terminated at the ultimate load, and it is not necessary to analyze the spread of damage following the formation of a collapse mechanism. While the proposed approach could be applied to more general damage scenarios, hazard-independent damage scenarios are considered in this study consisting of sudden loss of a single column at various locations in a building. As discussed by Gudmundsson and Izzuddin (2010), sudden column loss, while clearly an idealization, is a useful damage scenario that captures the dynamic nature of damaging events such as blast or impact and enables evaluation of a structure's capacity to absorb the additional energy associated with such dynamic events. Khandelwal and El Tawil (2011) presented an "incremental dynamic pushdown" approach to account for the dynamic effects associated with sudden column loss but noted the disadvantage that "this approach is costly in terms of required computational effort because multiple nonlinear, dynamic analyses must be conducted." This paper presents and verifies an energy-based procedure that accounts for such dynamic effects using the results of a single nonlinear static pushdown analysis, thus significantly reducing the required computational effort.

The proposed methodology for evaluation of robustness could be implemented using various levels of modeling sophistication. While many previous studies have analyzed planar frames, neglecting the effects of three-dimensional framing and floor slabs, these effects are known to contribute significantly to the robustness of reinforced concrete (RC) frame structures. In this study, the reduced-order modeling approach developed and validated by Bao et al. (2014a) for

two-dimensional RC frames without floor slabs is extended to incorporate a new reduced-order modeling approach for floor slabs within three-dimensional RC framing. Prior to outlining the proposed methodology for evaluation of structural robustness, the reduced-order modeling approach is outlined, and verification of the approach is presented through comparison with high-fidelity finite element model results from pushdown analysis of a 2-bay by 2-bay floor system. Comparisons of high-fidelity finite-element analysis results with and without the floor slab illustrate the significant contribution of the floor slabs in increasing the capacity of the framing under column loss and reducing the susceptibility to snap-through instability. The methodology is then demonstrated through application to 10-story prototype buildings using the reduced-order modeling approach, including floor-slab effects. A key observation from these analyses is that the robustness of multi-story buildings can be limited by column failure modes that would not be evident from analysis of a single-floor system. Another significant result of the prototype building analyses is a quantification of the extent to which structural robustness against column loss can be enhanced through the use of seismic design and detailing.

Slab Modeling in RC Floor Systems

Although a number of computational and experimental studies on the collapse resistance of RC subassemblies or planar frames have been reported in recent years (Sasani et al. 2011; Yu and Tan 2013; Bao et al. 2014a; Lew et al. 2014), experimental investigations on three-dimensional RC frame structures with floor slabs (e.g., Xiao et al. 2015) have been limited because of their cost and complexity. However, the importance of three-dimensional effects in evaluation of collapse resistance is recognized by design criteria such as the Unified Facilities Criteria 4-023-03 (DoD 2009), which prohibits the use of two-dimensional models. Studies of steel frame buildings have found that the floor slab contributes significantly to the collapse resistance of

structures (Sadek et al. 2008; Main 2014). It is a challenge to develop reliable models that can be used in the analysis of large-scale structures without imposing prohibitive computational costs. In this study, experimentally validated models of planar frames (Bao et al. 2014a) are extended to develop a reduced-order modeling approach for three-dimensional frame systems including floor slabs. In the absence of experimental data under the distributed pushdown loading conditions proposed for evaluation of structural robustness, The reduced-order modeling approach is verified through comparison with high-fidelity finite-element analysis results for a 2-bay by 2-bay floor system under center column loss. The objective of these comparisons is to verify that the reduced-order modeling approach can adequately capture the nonlinear load-displacement relationship and failure modes under distributed pushdown loading.

The design of the 2-bay by 2-bay floor system, shown in plan view in Fig. 1, was adapted from a half-scale, 3-story, 3-bay by 3-bay RC frame building tested under column removal scenarios by Xiao et al. (2015). A single floor was considered, with columns extending one half-story above and below. Table 2 lists beam reinforcement details, and Fig. 2 shows column reinforcement details. Slab reinforcement, both top and bottom, consisted of two layers of 8 mm diameter bars spaced at 200 mm (not shown). In both the reduced-order and high-fidelity models, the reinforcing steel was modeled using the piecewise-linear stress-strain curve illustrated in Fig. 3(a), with an assumed yield strength of f_y = 400 MPa, an ultimate strength of f_u = 520 MPa at a corresponding uniform strain of ε_u = 10 %, and an elongation of ε_f = 18 % at fracture. Values of elongation at fracture used in this study were based on tensile testing of reinforcing bars reported by Lew et al. (2011). The compressive strength of concrete was assumed to be f_c' = 25 MPa, while the reduced-order and high-fidelity models used different material modeling approaches for concrete, as described in the following sections.

Reduced-Order Modeling

The reduced-order modeling approach is illustrated in Fig. 4. The reduced-order model of the 2-bay by 2-bay floor system comprised approximately 1700 shell elements representing the floor slab and 230 beam elements representing the beams and columns. Nodes of the beam and shell elements were at the top surface of the slab, and offsets were used to define the reference axes of the elements at their proper elevations. Nodal constraints were used to tie the beam elements to the shell elements, ensuring continuity of displacements and rotations at the interface between the beams and the floor slab. The shell elements used through-thickness integration, with distinct layers for concrete and reinforcing steel. The beam elements used cross-section integration, with distinct integration points for core concrete, cover concrete, and reinforcing steel. Slab concrete and cover concrete were modeled using the unconfined stress-strain relationship shown in Fig. 3(b), with an assumed strain of ε_{c1} = 0.002 at the compressive strength f'_c. Confinement effects were incorporated in the stress-strain relationship for the core concrete using a modified Kent and Park model proposed by Scott et al. (1982), which accounted for the increased compressive strength f'_{cc} of the confined concrete as well as the increased strain at the compressive strength. Concrete softening behavior was considered in both tension and compression, and mesh-size dependence was controlled by using a constant fracture energy criterion, based on the element size, to calculate the ultimate strain at which the strength is reduced to zero ($\varepsilon_{u,c}$, $\varepsilon_{u,cc}$, and ε_u^{cr} in Figs. 3(b) and 3(c)), following the approach used by Bao et al. (2014a). Bond slip at critical cross sections, including the beam-to-column interfaces and the bar cut-off locations, was considered by using special interface elements at those locations. These interface elements (beam elements with cross-section integration) used a modified stress-strain relationship for the reinforcing bars developed by Bao et al. (2014a) that incorporated displacements due to bond slip. In both the interface elements and in the shell elements representing the slab, a critical plastic strain was

specified for the reinforcing bars, corresponding to the assumed elongation at fracture of ε_f = 18 %, at which the stress at the corresponding integration points dropped to zero, representing fracture of the reinforcing bars.

Modeling of the structural framing (beams and columns) followed the approach described by Bao et al. (2014a), with one significant simplification, that shear deformations of the joints were neglected. Bao et al. (2014a) used a planar macromodel approach to account for shear deformation of the joints, and Bao et al. (2014b) extended this approach to three-dimensional structures by considering shear deformations in three orthogonal planes. However, no significant contributions from joint shear deformations have been observed in previous experimental studies under column loss scenarios (Yi et al. 2008; Su et al. 2009; Yu and Tan 2013; Lew et al. 2014; Xiao et al. 2015), suggesting that the additional complexity of modeling such deformations may be unnecessary. Modeling the joint region as rigid, as proposed in this study, simplifies the model development process and reduces the computation time required for analysis. Analysis results from models of the 2-bay by 2-bay floor system with and without consideration of joint shear deformations, presented subsequently, confirmed that the effects of joint shear deformations were not significant.

High-Fidelity Modeling

The high-fidelity model of the 2-bay by 2-bay floor system, shown in Fig. 5, comprised approximately 217 000 elements in total, including beam elements representing reinforcing bars and solid elements representing concrete. This model followed the detailed modeling approach described by Bao et al. (2014a), which was validated against experimental data from two full-scale moment-frame assemblies tested under center column removal scenarios. The characteristic

length of solid elements representing concrete was between 20 mm and 35 mm. The length of beam elements representing reinforcing bars ranged from 45 mm to 120 mm. Bond slip between beam longitudinal bars and the surrounding concrete was modeled for the interior beams using a one-dimensional contact interface. Bond slip was not considered for the other reinforcing bars (i.e., stirrups, slab reinforcement, and longitudinal reinforcement in the columns and exterior beams); rather, the nodes of those reinforcing bar elements were tied to the surrounding concrete using constraints. A continuous surface cap model (Murray et al. 2007) was adopted for modeling concrete behavior. This model captures important features such as confinement effects and softening behavior in both tension and compression, and it uses a constant fracture energy approach to regulate mesh size sensitivity in the modeling of softening behavior. Reinforcing steel was modeled using an isotropic elastic-plastic model, using the stress-strain relationship illustrated in Fig. 3(a). A plastic strain at failure was also specified, corresponding to the assumed elongation of ε_f = 18 %. Once the failure strain was reached, the corresponding element was removed from the analysis (element erosion), representing fracture of the reinforcing bar.

Comparison of Analysis Results

In analyses of the 2-bay by 2-bay floor system (Fig. 1), the bases of the exterior columns were fixed, while the base of the center column was unsupported, representing a center column removal scenario. Horizontal displacements were restrained at the column tops. Uniformly distributed loading was applied to the floor slab, and using a force-controlled pushdown approach, the load intensity was gradually increased until failure occurred. The pushdown analyses in this study were performed using explicit time integration in the LS-DYNA finite-element software (Hallquist 2007), and the intensity of the force-controlled loading was increased at a sufficiently slow rate to ensure a quasi-static response prior to failure. The load

intensity was calculated by dividing the total vertical reaction at the column bases by the area of the floor slab that was subjected to pushdown loading.

Curves of load intensity versus vertical displacement of the unsupported center column are shown in Fig. 6 for both the reduced-order and the high-fidelity models. Results from two different reduced-order models are shown in Fig. 6: one in which joint shear deformations were considered using the approach of Bao et al. (2014b) and the other in which joint shear deformations were neglected as proposed in this study. The close agreement between the results of the two reduced-order models confirms that the effects of joint shear deformations were not significant. Fig. 6 also shows close agreement between the load-displacement relationships obtained from the reduced-order models and the high-fidelity model, providing verification of the reduced-order modeling approach. Contours of vertical displacement at the peak load intensity are shown in Fig. 7, which shows that the two modeling approaches gave fairly consistent predictions of the overall deflected shape, although some local differences in the displacement contours are evident. As illustrated in Fig. 8 using computed results from the high-fidelity model, failure of the floor system started with fracture of the top longitudinal bars at the ends of the short-span beams near the exterior columns, which was followed by the fracture of adjacent reinforcing bars in the slab. A consistent sequence of failures was evident in the reduced-order models, with failures being evident through reductions in stress at integration points representing the reinforcing bars in the beam and shell elements at the ends of the short-span beams near the exterior columns.

Fig. 9 shows the influence of the floor slab on the resistance of the 2-bay by 2-bay floor system by comparing pushdown analysis results from high-fidelity models with and without the floor slab. While structural analysis models used for the design of RC frame buildings typically

include only the framing, not the floor slabs, Fig. 9 shows that the additional resistance provided by the floor slab is significant, more than doubling the capacity of the system. Results for the system without floor slab were obtained by applying concentrated loading to the unsupported center column under displacement control. To enable a consistent comparison, results under concentrated loading are also presented for the system with floor slab, along with the results under uniform loading, which were previously presented in Fig. 6. The load intensity under concentrated loading was calculated by dividing the applied load by the tributary area of the center column (one quarter of the total floor area).

For the system with floor slab, Fig. 9 shows that the results under concentrated loading and uniform loading agreed quite closely when presented in terms of load intensity, as noted previously for steel/concrete composite floor systems by Alashker et al. (2010) and Main (2014). In contrast with the top bar failures observed under uniform loading, however (see Fig. 8), the first reinforcing bars to fracture under concentrated loading were the bottom bars in the short-span beams near the center column. The failure mode under concentrated loading was the same with and without the floor slab, although the failure occurred earlier – and at a much greater capacity – for the system with the floor slab. Fig. 9 shows that the system without the slab exhibited a softening phase, for center column displacements between approximately 70 mm and 300 mm, which was associated with crushing of concrete and yielding of reinforcing bars at the beam ends, as observed previously in planar frames by Lew et al. (2011). The additional resistance provided by the floor slab eliminated this softening phase, producing a monotonically increasing load-displacement relationship. Under force-controlled loading, the softening phase would result in snap-through instability, as illustrated in Fig. 9, with undesirable dynamic

amplification of loads. The influence of the floor slab, therefore, resulted in a system with both significantly increased capacity and improved energy absorption characteristics.

Prototype Building Designs

Two 10-story prototype buildings are used as examples to demonstrate the proposed robustness evaluation method in the following sections. The two buildings were designed for Seismic Design Categories C and D, using intermediate moment frames (IMFs) and special moment frames (SMFs), respectively, to resist seismic loads. Fig. 10 shows plan and elevation views, which were the same for both buildings, and Table 3 provides cross-section dimensions of the beams and columns. The slab thickness in both buildings was 254 mm. Further information on the prototype building designs is provided by Lew at al. (2011) and Shen and Ghosh (2006). The minimum specified compressive strength of $f_c' = 27.6$ MPa was assumed in modeling of concrete. The minimum specified yield and ultimate strengths of $f_y = 414$ MPa and $f_u = 620$ MPa were assumed in modeling of the ASTM A615 Grade 60 reinforcing bars, with $\varepsilon_u = 10$ % and $\varepsilon_f = 20$ % (see Fig. 3(a)). In evaluating the robustness of the prototype buildings, service-level gravity loading G was considered, based on the following load combination specified in ASCE 7-10 (ASCE 2010, Section 2.5.2.2) for evaluating the residual capacity of structural systems following the notional removal of load-bearing elements:

$$G = 1.2D + 0.5L \tag{1}$$

where D is dead load and L is live load. Table 4 summarizes the applicable gravity loads for the two prototype buildings. The combined gravity load G was greater for the SMF building than for the IMF building because of the greater self-weight associated with the larger member sizes.

Evaluation of Structural Robustness

In the proposed methodology for evaluating structural robustness, the first step is to identify a set of applicable damage scenarios to be considered. Damage scenarios may be specified by the building owner based on a risk analysis considering the relevant hazards, or they may be hazard-independent damage scenarios specified by an applicable code or standard. In this study, the damage scenarios are limited to loss of a single column. However, the methodology could be extended to other damage scenarios, such as the loss of load-bearing members within a specified damage volume, which could include a structural wall, multiple columns, or a portion of a beam or girder.

For each column loss scenario, the ultimate capacity is evaluated through nonlinear static pushdown analysis of the structure with the column removed, while an energy-based analysis is used to account for the dynamic effects associated with sudden column loss. The resulting ultimate capacity of the damaged structure, representing the peak vertical load intensity that can be sustained under sudden column loss, is divided by the service-level gravity loading G to obtain a normalized ultimate capacity for each column loss scenario. After considering all applicable column loss scenarios, the minimum value of the normalized ultimate capacity is designated as the robustness index for the structure. A robustness index greater than unity indicates that collapse would not occur under any of the applicable sudden column loss scenarios.

Further details on the robustness evaluation methodology are provided in the following subsections, including a formal definition of the robustness index, after introducing the relevant notation. The methodology is illustrated through analyses of a single-floor system extracted from the prototype IMF building (see Fig. 10 and Table 3) under loss of interior column C2. The reduced-order modeling approach was used in the analyses of the single-floor IMF system.

Similar to the boundary conditions considered previously for the 2-bay by 2-bay floor system, the columns were extended one half-story above and below the floor, and the column bases were fixed, with the exception of column C2, which was unsupported at its base, representing a column removal scenario. Horizontal displacements were restrained at the column tops. The robustness evaluation methodology is subsequently applied to both of the 10-story prototype buildings under multiple column loss scenarios.

Pushdown Analysis Procedure

In pushdown analysis of a structure under a column loss scenario, the column is removed prior to loading, and gravity loading is applied according to the pattern illustrated in Fig. 11. Service-level gravity loading G is first applied to the bays not directly affected by the column loss and is held constant for the remainder of the analysis. Scaled gravity loading $\lambda_s G$ is then applied to the affected bays, and the pushdown analysis is performed by increasing the dimensionless factor λ_s from zero until the ultimate capacity is reached. The affected bays are defined by the influence area of the removed column, where the influence area is "that portion of the floor area over which the influence surface for structural effects is significantly different from zero" (ASCE 2010, Section C4.7.1). Fig. 12 illustrates the affected bays for other column removal scenarios in the prototype buildings, and further explanation and examples for evaluation of influence areas can be found in the Appendix of ASCE 7-10 (ASCE 2010, Section C4.7.1). The scaled gravity loading $\lambda_s G$ is applied to the affected bays on all floors above the removed column. The dimensionless factor λ_s, where the subscript indicates *static* loading, represents the normalized load intensity applied to the affected bays, with $\lambda_s > 1$ indicating loads in excess of the service-level gravity loading. In the nonlinear static pushdown analysis, the dimensionless factor λ_s is

increased from zero until the ultimate capacity is reached. The relationship between the normalized load intensity and the vertical displacement Δ at the removed column is thus obtained, denoted by $\lambda_s(\Delta)$, as illustrated in Fig. 13 for the single-floor IMF system subjected to removal of column C2.

In the terminology of Khandelwal and El-Tawil (2011), the proposed pushdown loading procedure (Fig. 11) constitutes a "bay pushdown" approach, in contrast with a "uniform pushdown" approach, in which the gravity loading would be increased uniformly over the entire floor area. Khandelwal and El-Tawil (2011) did not consider dynamic effects in either the bay pushdown approach or the uniform pushdown approach. In the proposed approach, however, dynamic effects associated with sudden column loss are accounted for through an energy-based analysis, as discussed in the following section. When using this energy-based analysis, the bay pushdown approach has the advantage that these dynamic effects are accounted for by the increased gravity loading on the affected bays. No such dynamic effects justify the application of increased gravity loads to the unaffected bays, and artificially increasing these loads can result in failure modes that may not be relevant to the column removal scenario under consideration. For example, the uniform pushdown approach can produce unrealistically large column forces, resulting in column failures that would not occur under sudden column loss. In the proposed bay pushdown approach, axial forces in columns at the boundary between affected and unaffected bays are scaled by an effective factor of less than λ_s, as they receive loading of intensity G from unaffected bays on one side and loading of intensity $\lambda_s G$ from affected bays on the other side. As is shown subsequently, the proposed bay pushdown approach, coupled with an energy-based analysis, provides good agreement with direct dynamic analyses of sudden column loss.

Energy-Based Analysis of Sudden Column Loss

Given a load-displacement relationship obtained from static pushdown analysis of a structure with a missing column, energy-based analysis can be used to account for the dynamic effects associated with sudden column loss (Powell 2003; Izzuddin et al. 2008; Xu and Ellingwood 2012; Main 2014). The analysis is based on the fact that the kinetic energy is zero at the peak dynamic displacement following the sudden loss of a column, assuming a single predominant mode of deformation and assuming that the gravity loads are not sufficient to cause collapse. Conservation of energy at the peak displacement then requires the internal energy in the structure to equal the external work done by gravity loads. The solid curve in Fig. 14 illustrates the results of a static pushdown analysis, representing the relationship between the normalized load intensity and the vertical displacement at the removed column, denoted by $\lambda_s(\Delta)$. Let $\lambda_d(\Delta)$ (illustrated by the dashed curve in Fig. 14) denote the corresponding relationship between the normalized load intensity and the peak dynamic displacement under sudden column loss. At a peak dynamic displacement of Δ, the balance between the work done by the external gravity loads (proportional to the hatched area in Fig. 14) and the internal energy in the structure (proportional to the shaded area in Fig. 14) can be expressed as follows:

$$\lambda_d(\Delta)\cdot\Delta = \int_0^{\Delta} \lambda_s(\tilde{\Delta})d\tilde{\Delta} \tag{2}$$

where $\tilde{\Delta}$ is a dummy variable in the integral representing the vertical displacement at the removed column. Rearranging Eq. (2) yields the following expression for $\lambda_d(\Delta)$.

$$\lambda_d(\Delta) = \frac{1}{\Delta}\int_0^{\Delta} \lambda_s(\tilde{\Delta})d\tilde{\Delta} \tag{3}$$

Eq. (3) allows the dynamic effects associated with sudden column loss to be evaluated directly from the results of a nonlinear static pushdown analysis. Eq. (3) was used to obtain the dashed

curve in Fig. 13, which shows the relationship between the normalized load intensity and the peak dynamic displacement after sudden column loss for the single-floor IMF system.

The dynamic increase factor at a given column displacement can be defined as the ratio between the normalized load intensities under static loading and under sudden column loss:

$$\Omega(\Delta) = \frac{\lambda_{\mathrm{s}}(\Delta)}{\lambda_{\mathrm{d}}(\Delta)} = \frac{\lambda_{\mathrm{s}}(\Delta)\cdot\Delta}{\int_0^{\Delta}\lambda_{\mathrm{s}}(\tilde{\Delta})d\tilde{\Delta}} \tag{4}$$

in which the latter expression results from substitution of $\lambda_{\mathrm{d}}(\Delta)$ from Eq. (3). Eq. (4) admits a simple geometric interpretation with reference to Fig. 14, in which the denominator is represented by the shaded area, and the numerator is represented by area of the bounding rectangle (indicated by dashed red lines) that encloses this shaded area. For a linear response, the shaded area is triangular and encompasses exactly half of the bounding rectangle, so that $\Omega = 2$. As the structure loses stiffness and the load-displacement relationship develops downward concavity, as illustrated in Fig. 14, the shaded area encompasses more than half of the bounding rectangle, so that values of $\Omega < 2$ are obtained. For an idealized elastic, perfectly plastic system, the shaded area would converge to fill the bounding rectangle as the displacement becomes large relative to the yield displacement, so that Ω would decrease to approach unity with increasing plastic deformation. Since the proposed procedure evaluates structural robustness from the normalized ultimate capacities under sudden column loss, rather than under static loading, the dynamic increase factor, which results from the shape of the load-displacement relationship, has a significant influence on the robustness of a structure.

The approximate energy-based analysis is based on the assumption that the structure responds in a single predominant deformation mode that is the same under both static loading and sudden column loss. To verify the accuracy of the energy-based analysis, results from this

procedure were compared with results from direct dynamic analysis of the single-floor IMF system under sudden loss of column C2. In the direct dynamic analyses, gravity loading was gradually applied to the floor system over a period of 3 s using a smooth ramp function and was held constant for an additional 0.5 s to avoid introduction of spurious dynamic effects. After the gravity initialization (i.e., at t = 3.5 s) column C2 was removed instantaneously, and the peak dynamic displacement was obtained from the analysis. By repeating this analysis procedure for increasing levels of gravity loading, using an incremental dynamic analysis approach, discrete points representing various normalized load intensities and the corresponding peak displacements could be obtained, which are plotted with open circles in Fig. 13. Gravity loading was varied only on the bays directly affected by loss of column C2 (see Fig. 11), and the service-level gravity loading G was applied to the unaffected bays. Different values of gravity load intensity were achieved in the reduced-order model by adding distributed mass to the floor system, and gravity loading was applied by imposing body forces due to gravitational acceleration. This approach properly accounted for both the gravity loading and inertial effects on the structure. Fig. 13 shows excellent agreement between the results of the energy-based analysis and the direct dynamic analysis of sudden column loss, providing verification of the energy-based approach. The energy-based analysis procedure offers a significant advantage in terms of efficiency, because it requires only a single static pushdown analysis, whereas the direct dynamic analysis approach requires multiple dynamic analyses to be performed at different load intensities.

Ultimate Capacity under Sudden Column Loss

Letting $\lambda_{s,u} = \lambda_s(\Delta_u)$ denote the ultimate value of the normalized load intensity obtained from a static pushdown analysis (see Fig. 13), the corresponding displacement Δ_u is proposed as the

limiting deflection at which the ultimate capacity under sudden column loss is evaluated. Fig. 13 shows that $\lambda_d(\Delta)$ continues to increase for displacements exceeding Δ_u as a result of residual, post-ultimate resistance of the structural system. Provided that $\lambda_s(\Delta) > \lambda_d(\Delta) > 1$, the energy-based analysis predicts that collapse will not occur. However, the assumption in the energy-based analysis of a single, unchanging deformation mode is generally not appropriate for displacements exceeding Δ_u, because the drop in resistance at this point is generally associated with the formation of a collapse mechanism. In addition, uncertainties in model predictions increase significantly in the post-ultimate descending portion of the static pushdown curve, which corresponds to the onset of a dynamic collapse process, in which unbalanced loads from the force-controlled loading procedure cause the structure to accelerate downward. For these reasons, it is prudent to conservatively evaluate the normalized ultimate capacity under sudden column loss at the displacement Δ_u, as follows (see Fig. 13).

$$\lambda_{d,u} = \lambda_d(\Delta_u) \tag{5}$$

Using this energy-based approach, a normalized ultimate capacity of $\lambda_{d,u} = 2.66$ was obtained for the single-floor IMF system under sudden loss of column C2 (plotted with a solid circle in Fig. 13), which is 3.3 % less than the normalized ultimate capacity of 2.75 obtained from direct dynamic analysis (the rightmost open circle in Fig. 13). In this example, as in the other examples considered subsequently, the proposed ultimate capacity estimate using energy-based analysis is found to be slightly conservative.

Using the procedures outlined above, the normalized ultimate capacity under sudden column loss can be evaluated for each column removal scenario, denoted by $\lambda_{d,u}^{i}$, where the superscript

denotes the ith column removal scenario. The robustness index R is then obtained as the minimum value of the normalized ultimate capacity over all column removal scenarios:

$$R = \min_i \left(\lambda_{\mathrm{d,u}}^{i} \middle| \, i \in \text{column removal scenarios} \right) \tag{6}$$

Robustness Evaluation of Prototype Buildings

The two 10-story prototype buildings (Fig. 10) are used as examples to demonstrate the proposed robustness evaluation methodology. Noting the double symmetry of the floor plan, it was sufficient to consider column removal scenarios in only one quadrant of the building, and the seven columns in the northwest quadrant of the building were selected for removal: A1, A2, A3, B1, C1, C2, and C3. In each of the seven column removal scenarios, removal of a single column was considered at the first-story level. The affected areas, on which the scaled gravity loading $\lambda_s G$ was applied for all floors (including the roof), are illustrated in Figs. 11 and 12.

Fig. 15 presents analysis results for both the IMF building and the SMF building subject to removal of column C2. Comparison of Fig. 14(a) to Fig. 13, which presented results for a single floor from the same building under the same column removal scenario, shows that the 10-story building sustained significantly smaller load intensities, with much smaller displacements prior to failure. For the 10-story building, the normalized ultimate capacity under sudden column loss was $\lambda_{\mathrm{d,u}}$ = 1.13, with a corresponding displacement of Δ_{u} = 75 mm at the ultimate static load, whereas values of $\lambda_{\mathrm{d,u}}$ = 2.66 and Δ_{u} = 1420 mm were obtained for the single-floor system. The reason for the lower capacity of the 10-story building is that the governing failure mode was compressive failure of a column, due to accumulation of gravity loads over the height of the building, rather than failure of the floor system itself. For both the IMF and the SMF buildings subjected to removal of column C2, the ultimate static capacity under pushdown loading was

associated with compressive failure of column A2, which was adjacent to the removed column on the exterior of the building, with failure occurring in the first story for the IMF building (see Fig. 16) and in the second story for the SMF building.

Contours of vertical displacement obtained from pushdown analysis of the IMF building are presented in Fig. 16. Fig. 16(a) shows displacement contours just prior to failure of column A2, corresponding to the ultimate capacity under static loading at Δ_u = 75 mm, while Fig. 16(b) shows displacement contours after the failure of column A2, for Δ = 220 mm. Comparison of Figs. 16(a) and 16(b) shows that the failure of column A2 produced a significant change in the deformation mode, with substantially increased vertical displacements above the failed column A2, where vertical displacements had previously been near zero. This change in the deformation mode invalidates a key assumption in the energy-based analysis procedure and confirms the appropriateness of limiting the application of this procedure to displacements not exceeding Δ_u, according to Eq. (5). Comparison with results from direct dynamic analysis of sudden column loss shows that the energy-based procedure was slightly conservative prior to Δ_u, with the dashed curves falling below the open circles in Fig. 15, but was not conservative after Δ_u, with the dashed curve increasing well beyond the highest load intensity sustained in the dynamic analyses. Under direct dynamic analysis of sudden column loss, the largest normalized load intensities that were sustained without collapse were 1.28 for the IMF building and 1.85 for the SMF building. The corresponding energy-based estimates of the normalized ultimate capacities under sudden column loss ($\lambda_{d,u}$ = 1.13 for the IMF building and $\lambda_{d,u}$ = 1.82 for the SMF building) were less than these values by 12 % and by 2 % respectively, confirming that for these examples, the proposed approach, using Eq. (5), is slightly conservative.

Table 5 lists analysis results for each of the seven column removal scenarios considered, for both the IMF building and the SMF building. Normalized ultimate capacities are presented for both static pushdown loading ($\lambda_{s,u}$) and sudden column loss ($\lambda_{d,u}$), as well as the ratio between these two capacities, which gives the dynamic increase factor at the displacement Δ_u: $\Omega(\Delta_u) = \lambda_{s,u} / \lambda_{d,u}$. The dynamic increase factor Ω, obtained from Eq. (4), is also plotted with the analysis results in Fig. 15, as a function of the displacement Δ at the removed column C2. As discussed previously in relation to Eq. (4), $\Omega = 2$ in the initial elastic response, and Ω decreases as the stiffness of the system degrades. Values of $\Omega(\Delta_u)$ ranged from 1.18 to 1.61 for the IMF building and from 1.17 to 1.49 for the SMF building. These results indicate that there is significant variability in the dynamic increase factor even for the same building, depending on the type of structural response and the governing failure mode. The largest value of $\Omega(\Delta_u)$ for both buildings corresponded to removal of column C2, for which column failure occurred. Removal of column C2 also resulted in the minimum value of the normalized ultimate capacity under sudden column loss, $\lambda_{d,u}$, for both buildings. According to Eq. (6), the robustness index for the building is taken as the minimum value of $\lambda_{d,u}$ over all column removal scenarios, and robustness indices of $R = 1.13$ and $R = 1.82$ are thus obtained for the IMF and SMF buildings, respectively. For both of the buildings, $R > 1$, which indicates that collapse would not occur under sudden column loss for any of the column removal scenarios. The larger value of the robustness index for the SMF building indicates that the more stringent seismic design and detailing of the SMF building resulted in improved robustness against column loss relative to the IMF building.

Conclusions

A methodology for evaluating structural robustness was proposed that involves (1) identifying a set of column removal scenarios for consideration (or initial damage scenarios, more generally), (2) performing a nonlinear static pushdown analysis for each scenario, (3) using an energy-based analysis procedure to determine the approximate ultimate capacity under sudden column loss for each scenario, (4) normalizing the ultimate capacities by the applicable gravity loading, $G = 1.2D + 0.5L$, and (5) defining the minimum value of the normalized ultimate capacity under sudden column loss as the robustness index R for the structure. Application of the proposed methodology was demonstrated using reduced-order models of RC frame buildings that included the floor slabs, and comparisons with high-fidelity finite-element analysis results were presented to provide verification of the reduced-order modeling approach. Based on the analysis results presented in this study, the following main conclusions were reached:

- High-fidelity finite element analysis of a 2-bay by 2-bay floor system with and without the floor slab showed that the influence of the slab more than doubled the load intensity that could be sustained under pushdown loading with an unsupported center column.
- Shear deformations of the joints were found not to contribute significantly to the response of RC frame structures under column loss. Based on this observation, joints were modeled as rigid in the proposed reduced-order approach, while still accounting for nonlinearities at the beam-to-column interface. This approach greatly simplified the model development process and significantly reduced the computation time required for analysis.
- The energy-based procedure for analysis of sudden column loss was found to give good agreement with results from direct dynamic analysis, both for a single-floor system and for the 10-story prototype buildings. A “bay pushdown” approach was found to be preferable to

a “uniform pushdown” approach to properly capture dynamic amplification in the affected bays without the potential to produce irrelevant column failures through artificial amplification of gravity loads on unaffected bays.

- Dynamic increase factors corresponding to the ultimate capacities varied significantly, even for the same building, with values ranging from 1.18 to 1.61 for the IMF building and from 1.17 to 1.49 for the SMF building. Clearly the use of a constant dynamic increase factor for a particular type of structure would be inappropriate. The energy-based procedure provides a straightforward means of accounting for this variability, as influenced by the type of structural response and the governing failure mode, using static pushdown analysis results.
- The energy-based procedure was based on the assumption of an unchanging deformation mode, and the procedure was found to give non-conservative results in the post-ultimate response, when failures caused the collapse mode to change. Therefore, it was proposed to evaluate the ultimate capacity under sudden column loss at the displacement corresponding to the ultimate static load.
- The capacity of the 10-story IMF building under sudden column loss was found to be less than half of the capacity of a single-floor system extracted from the same building, because the governing failure mode was column failure rather than failure of the floor system. It is important to recognize that accumulation of gravity loads over the height of a multi-story building could result in column failures that would not occur in a single-floor system.
- Robustness indices of R = 1.13 and R = 1.82 were obtained for the prototype IMF and SMF buildings. For both buildings, $R > 1$, indicating that collapse would not occur under any of the sudden column removal scenarios. The larger value of the robustness index for the SMF

building also showed that the more stringent seismic design and detailing of the SMF building resulted in improved robustness against column loss relative to the IMF building.

Acknowledgements

Valuable comments and input on this work were provided by Fahim Sadek, H.S. Lew, and Jonathan M. Weigand of the National Institute of Standards and Technology.

Disclaimer

Certain commercial entities, equipment, products, or materials are identified in this document in order to describe a procedure or concept adequately. Such identification is not intended to imply recommendation, endorsement, or implication that the entities products, material, or equipment are necessarily the best available for the purpose.

References

Alexander, S. (2004). "New approach to disproportionate collapse." *The Struct. Eng.*, 82(3), 14-18.

American Society of Civil Engineers (ASCE). (2010). "Minimum design loads for buildings and other structures." *ASCE/SEI 7-10*, Reston, VA

Baker, J. W., Schubert, M., and Faber, M. H. (2008). "On the assessment of robustness." Structural Safety, 30(3), 253-267.

Bao, Y., Lew, H. S., and Kunnath, S. K. (2014a). "Modeling of reinforced concrete assemblies under column removal scenario." *J. Struct. Eng.*, 140(1), 04013026.

Bao, Y., Main, J. A., Lew, H. S., and Sadek, F. (2014b). "Robustness assessment of RC Frame Buildings under column loss scenarios." *Proc., 2014 Structures Congress*, Pittsburg, PA.

European Committee for Standardization (CEN). (2006). “Actions on structures. Part 1-7: Accidental actions.” *Eurocode 1, Part 1-7*, Brussels, Belgium..

Centre for the Protection of National Infrastructure. (2011). “Review of international research on structural robustness and disproportionate collapse.” London, UK.

Cranford, S. W., Tarakanova, A., Pugno, N. M., and Buehler, M. J. (2012). “Nonlinear material behaviour of spider silk yields robust webs.” *Nature*, 482, 72-76.

Department of Defense. (2009). “Design of buildings to resist progressive collapse.” UFC 4-023-03, Washington, DC.

Fascetti, A., Kunnath, S. K., and Nisticò, N. (2015). “Robustness evaluation of RC frame buildings to progressive collapse.” *Eng. Struct.*, 86, 242-249.

Foley, C. M. (2008). “Characteristics of robustness structures.” *Proc., North American Steel Construction Conf.*, Nashville, TN.

Formisano, A., Landolfo, R., and Mazzolani, F. M. (2015). “Robustness assessment approaches for steel framed structures under catastrophic events.” *Comp. Struct.*, 147, 216-228.

General Services Administration. (2003). “Progressive collapse analysis design guidelines for new federal office buildings and major modernization projects.” Washington, DC.

Gudmundsson, G. V., and Izzuddin, B. A. (2010). “The ‘sudden column loss’ idealisation for disproportionate collapse assessment.” *The Structural Engineer: Journal of the Institution of Structural Engineers*, 88(6), 22-26.

Hallquist, J. (2007). *LS-DYNA keyword user’s manual*, Livermore Software Technology Corporation, Livermore, CA.

Izzuddin, B. A., Vlassis, A. G., Elghazouli, A. Y., and Nethercot, D. A. (2008). "Progressive collapse of multi-storey buildings due to sudden column loss – Part I: Simplified assessment framework." *Eng. Struct.*, 30, 1308-1318.

Joint Committee in Structural Safety. (2001). *Probabilistic model code*.

Khandelwal K. and El-Tawil, S. (2011). "Pushdown resistance as a measure of robustness in progressive collapse analysis." *Eng. Struct.*, 33, 2653-2661.

Lew, H.S., Bao, Y., Pujol, S., and Sozen, M.A. (2014). "Experimental study of reinforced concrete assemblies under column removal scenario." *ACI Struct. J.*, 111(4), 881-892.

Lew, H.S., Bao, Y., Sadek, F. Main, A. J., Pujol, S., and Sozen, M. A. (2011). "An experimental and computational study of reinforced concrete assemblies under a column removal scenario." *NIST TN 1720*, National Institute of Standards and Technology, Gaithersburg, MD.

Lu, D. G., Cui, S. S., Song, P. Y. and Chen, Z. H. (2010). "Robustness assessment for progressive collapse of framed structures using pushdown analysis method." *Proc., 4th Intl. Workshop on Reliable Engineering Computing (REC)*, Singapore.

Main, J. A. (2014). "Composite floor systems under column loss: collapse resistance and tie force requirements." *J. Struct. Eng.*, 140, Special Issue: Computational Simulation in Structural Engineering, A4014003.

Murray, Y. D., Abu-Odeh, A., and Bligh, R. (2007). "Evaluation of LS-DYNA concrete material model 159." FHWA-HRT-05-063, Federal Highway Administration, McLean, VA.

Powell, G. (2003). "Collapse analysis made easy (more or less)." *Proc., Annual Meeting of the Los Angeles Tall Buildings Structural Design Council: Progressive collapse and blast resistant design of buildings*, Los Angeles, CA.

Powell, G. (2009). “Disproportionate collapse: The futility of using nonlinear analysis.” *Proc., 2009 Structures Congress*, Austin, TX.

Raebel, C. H. (2011). *A quantitative study of robustness characteristics in steel framed structures*, Dissertation, Marquette University, Milwaukee, WI.

Sadek, F., El-Tawil, S., and Lew, H. S. (2008). “Robustness of composite floor systems with shear tab connections: modeling, simulation, and evaluation.” *J. Struct. Eng.*, 134(11), 1717-1725.

Sasani, M., Werner, A., and Kazemi, A. (2011). “Bar fracture modeling in progressive collapse analysis of reinforced concrete structures.” *Eng. Struct.*, 33, 401-409.

Scott, B.D., Park, R., and Priestley, M.J.N. (1982) “Stress-strain behavior of concrete confined by overlapping hoops at low and high strain rates.” *ACI Journal*, 79(1), 13-27.

Shen, Q. and Ghosh, S. K. (2006). “Assessing ability of seismic structural systems to withstand progressive collapse: Progressive collapse analysis of cast-in-place concrete frame buildings.” *Report submitted to the National Institute of Technology*, Gaithersburg, MD.

Starossek, U. and Haberland, M. (2009). “Evaluating measures of structural robustness.” *Proc., 2009 Structures Congress*, Austin, TX.

Starossek, U. and Haberland, M. (2010). “Disproportionate collapse: Terminology and procedures.” *Journal of the Performance of Constructed Facilities*, 24(6), 519-528.

Su, Y., Tian, Y., and Song, X. (2009). “Progressive collapse resistance of axially-restrained frame beams.” *ACI Struct. J.*, 106(5), 600-607.

Xiao, Y., Kunnath, S. K., Li, F. W., Zhao, Y. B., Lew, H. S., and Bao, Y. “Collapse test of a 3-story 3-span half-scale reinforced concrete frame building.” *ACI Struct. J.* (in press)

Xu, G. and Ellingwood, B. R. (2012). “An energy-based partial pushdown analysis for robustness assessment of building structures.” *Proc., 2012 Structures Congress*, Chicago, IL.

Yu, J. and Tan, K.H. (2013). “Experimental and numerical investigation on progressive collapse resistance of reinforced concrete beam column sub-assemblies.” *Eng. Struct.*, 55, 90-106.

Table 1. Definitions of structural robustness

Source	Definition
GSA (2003)	"Ability of a structure or structural components to resist damage without premature and/or brittle failure due to events like explosions, impacts, fire or consequences of human error, due to its vigorous strength and toughness."
CEN (2006)	"The ability of a structure to withstand events like fire, explosions, impact or the consequences of human error, without being damaged to an extent disproportionate to the original cause."

Table 2. Beam reinforcement details for 2-bay by 2-bay floor system (units in mm)

Beam	Top reinforcement		Bottom reinforcement		Stirrups	
Dimensions	Ends	Middle	Ends	Middle	Ends	Middle
225 × 355	four ⌀12	three ⌀12	three ⌀12	seven ⌀12*	⌀8 @150	⌀8 @225
200 × 280	three ⌀12	three ⌀10	three ⌀10	three ⌀12	⌀8 @150	⌀8 @225
225 × 355	four ⌀12	three ⌀12	three ⌀12	seven ⌀12*	⌀8 @150	⌀8 @150

Note: Values following ⌀ indicate bar diameter; values following @ indicate bar spacing.
* Two layers of longitudinal reinforcement.

Table 3. Cross-section dimensions for beams and columns in 10-story prototype buildings

	Cross-section dimensions (mm)	
Frame members	IMF building	SMF building
Exterior columns	711 × 711	864 × 864
Interior columns	864 × 864	965 × 965
Exterior beams	711 × 508	864 × 660
Interior beams: E-W	711 × 508	864 × 660
Interior beams: N-S	864 × 762	965 × 813

Table 4. Gravity loads for prototype buildings

Gravity load type	IMF building		SMF building	
	Floors	Roof	Floors	Roof
Self-weight (kN/m^2)	7.18	7.18	8.14	8.14
Superimposed dead load (kN/m^2)	1.44	0.48	1.44	0.48
Total dead load, D (kN/m^2)	8.62	7.66	9.58	8.62
Live load, L (kN/m^2)	4.79	1.20	4.79	1.20
Combined gravity load, G (kN/m^2)	12.74	9.79	13.89	10.94

Table 5. Ultimate capacities and robustness indices for prototype buildings

Column removal scenario	IMF building			SMF building		
	Normalized ultimate capacity		Dynamic increase factor, $\Omega(\Delta_u)$	Normalized ultimate capacity		Dynamic increase factor, $\Omega(\Delta_u)$
	Static pushdown, $\lambda_{s,u}$	Sudden column loss, $\lambda_{d,u}$		Static pushdown, $\lambda_{s,u}$	Sudden column loss, $\lambda_{d,u}$	
A1	3.81	3.23	1.18	5.19	4.44	1.17
A2	2.01	1.69	1.19	3.17	2.62	1.21
A3	2.06	1.70	1.21	3.69	2.73	1.35
B1	2.74	1.94	1.41	4.64	3.93	1.18
C1	3.51	2.90	1.21	6.45	4.54	1.42
C2	1.82	1.13*	1.61	2.71	1.82*	1.49
C3	1.81	1.14	1.59	2.78	2.34	1.19

* The minimum value of $\lambda_{d,u}$ over all column removal scenarios defines the robustness index for the building, and values of R = 1.13 and R = 1.82 are obtained for the IMF and SMF buildings, respectively.

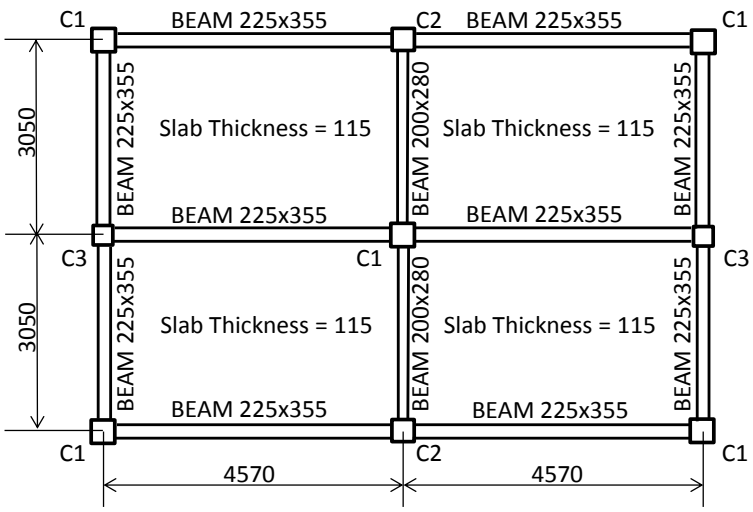

Fig. 1. Plan view of 2-bay by 2-bay floor system (units in mm)

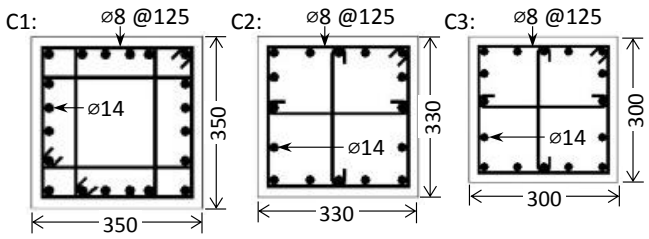

Fig. 2. Column reinforcement details for 2-bay by 2-bay floor system (units in mm)

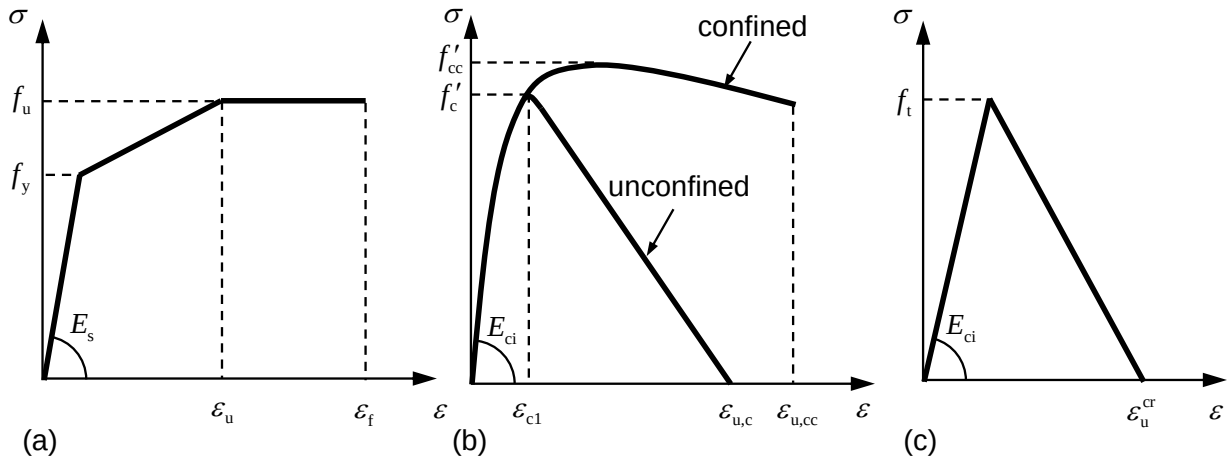

Fig. 3. Stress-strain relationships used in material modeling: (a) steel; (b) concrete in compression; (c) concrete in tension

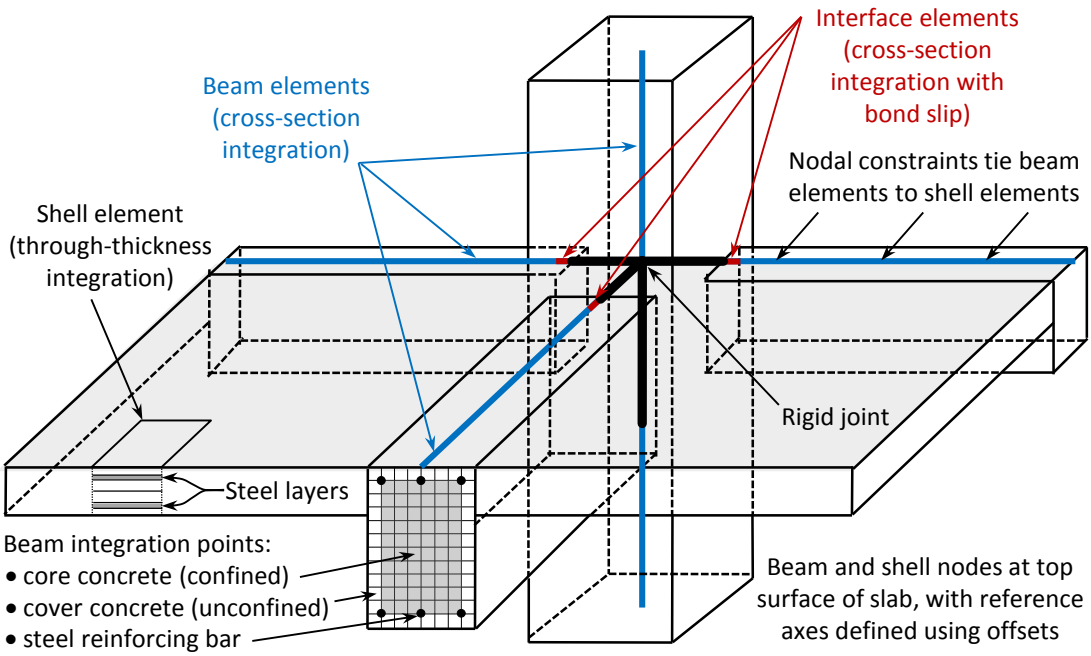

Fig. 4. Reduced-order modeling approach

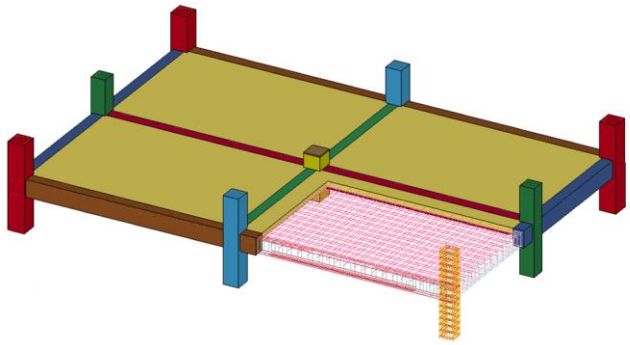

Fig. 5. High-fidelity model of 2-bay by 2-bay floor system

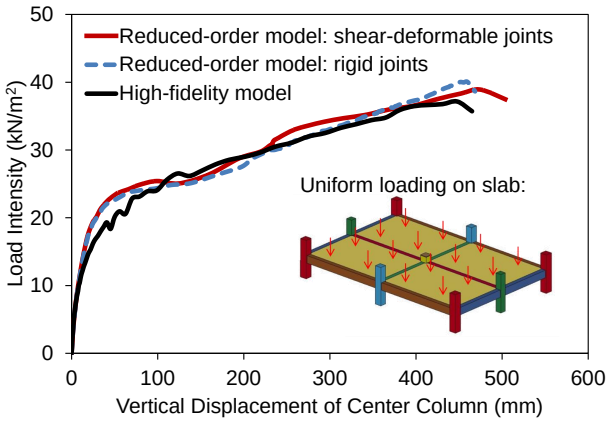

Fig. 6. Comparison of high-fidelity and reduced-order pushdown analysis results for 2-bay by 2-bay floor system

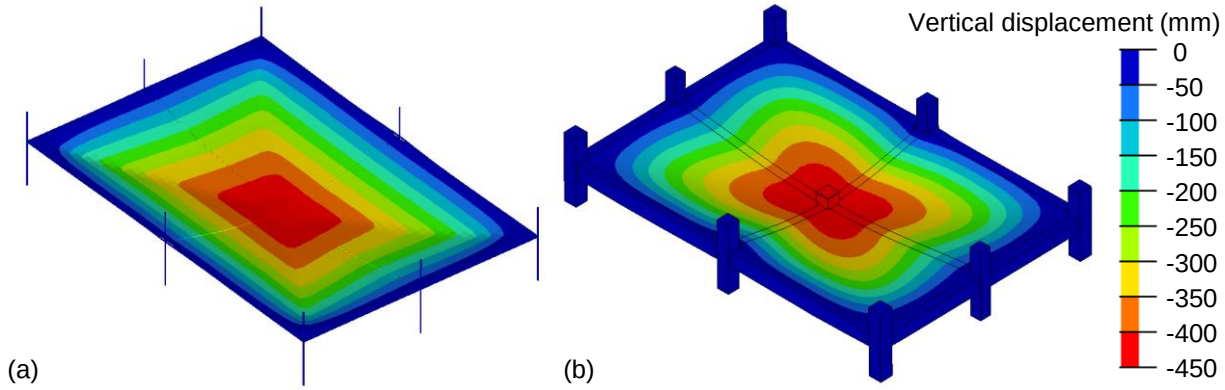

Fig. 7. Contours of vertical displacement at peak load intensity: (a) reduced-order model; (b) high-fidelity model

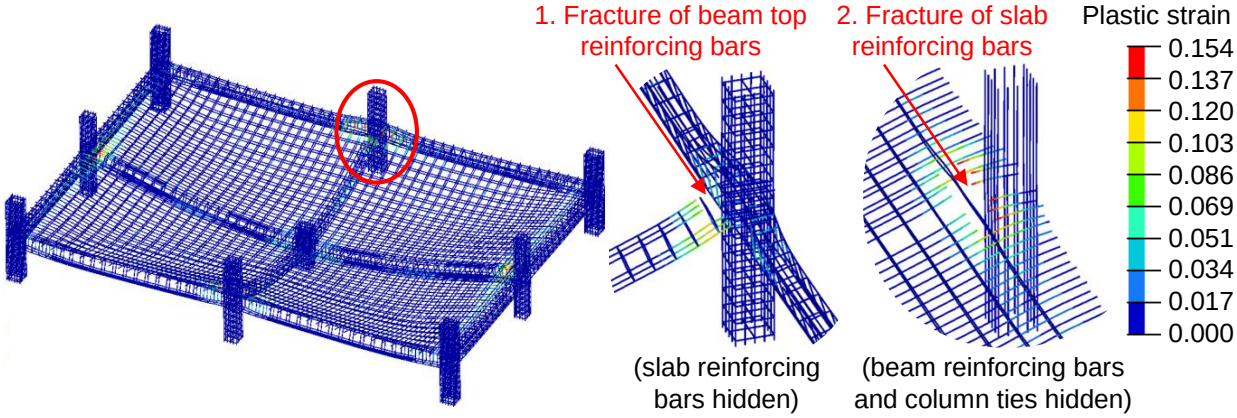

Fig. 8. Failure modes observed in high-fidelity model

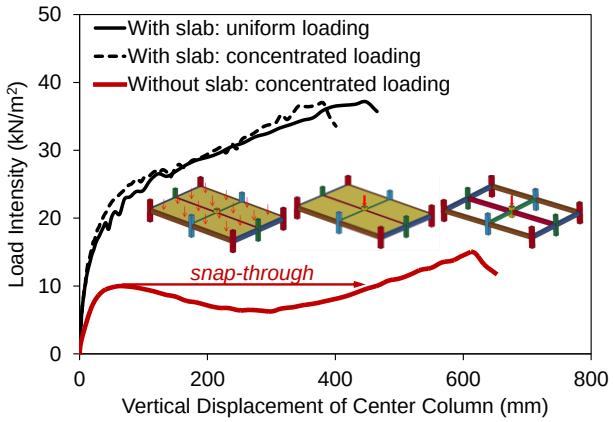

Fig. 9. Influence of floor slab on pushdown analysis results for 2-bay by 2-bay floor system

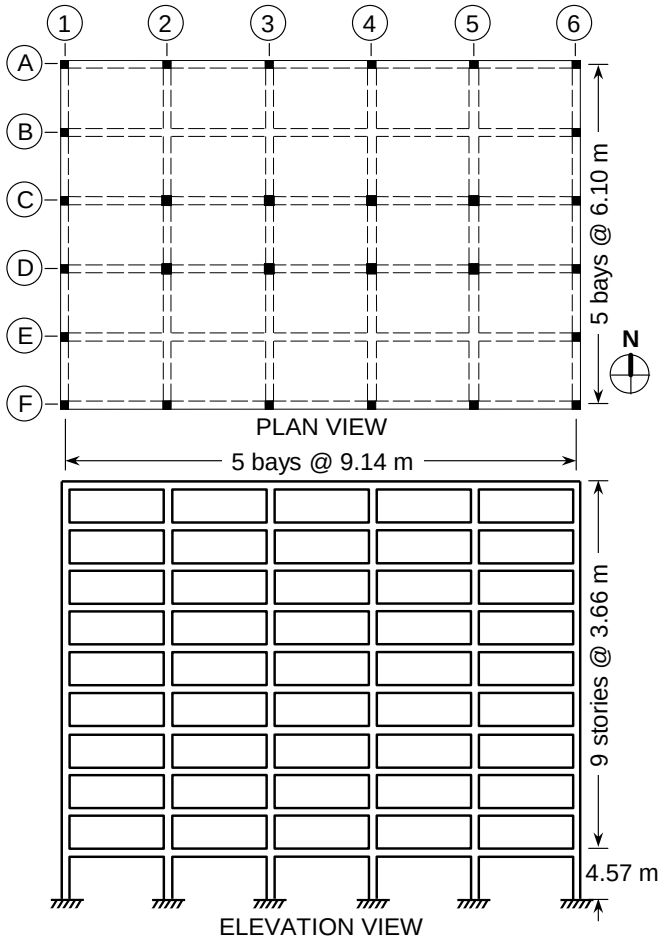

Fig. 10. Plan and elevation views of 10-story prototype buildings

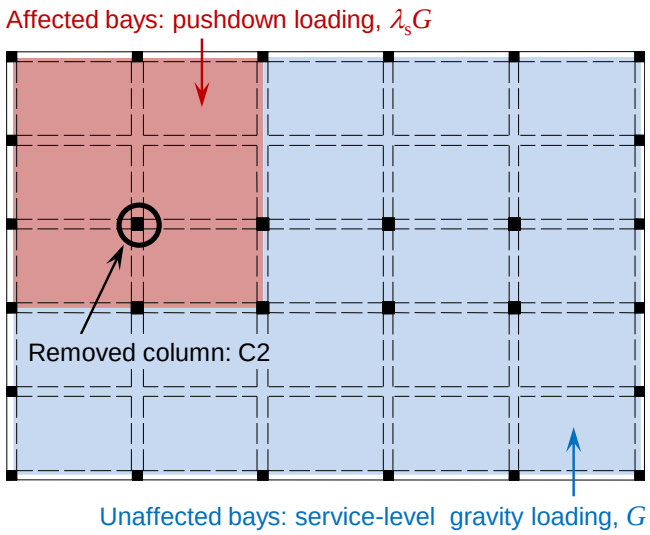

Fig. 11. Gravity load pattern for pushdown analysis

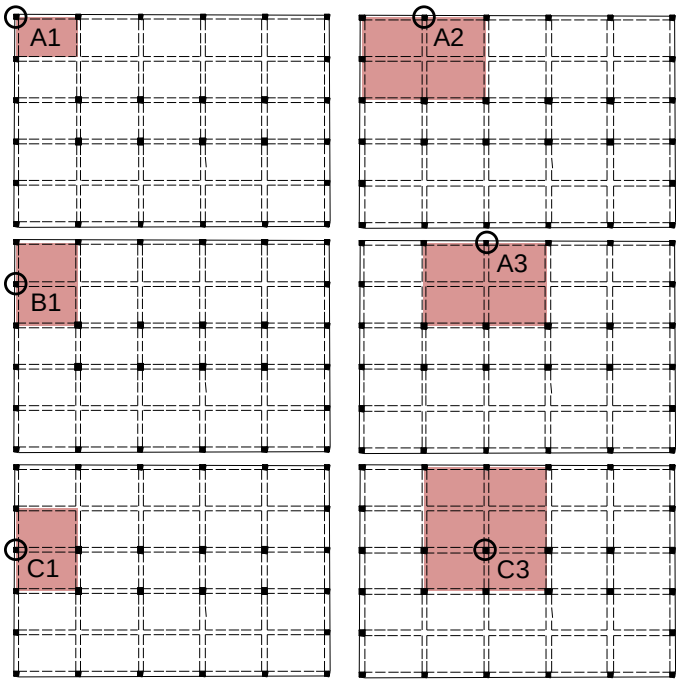

Fig. 12. Affected bays (column influence areas) for different column removal scenarios.

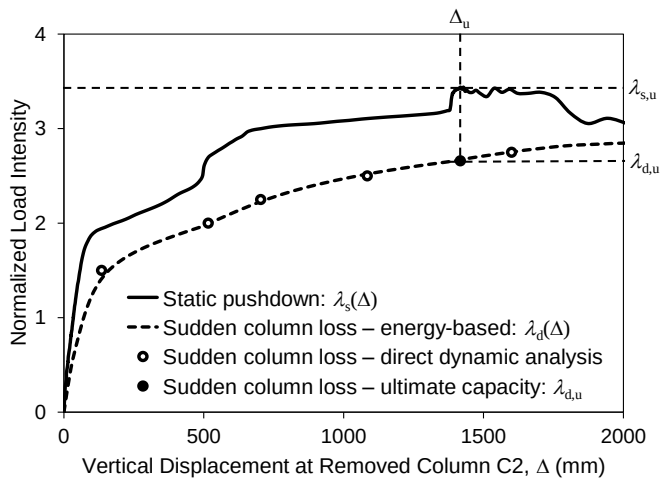

Fig. 13. Analysis results for the single-floor IMF system

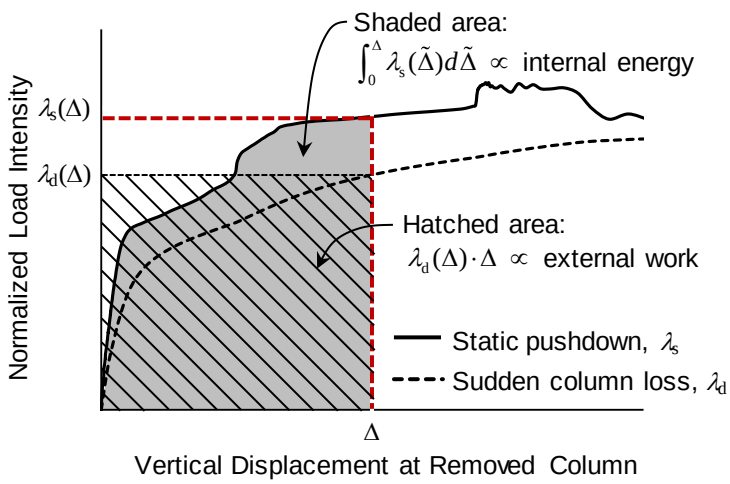

Fig. 14. Energy-based analysis of sudden column loss

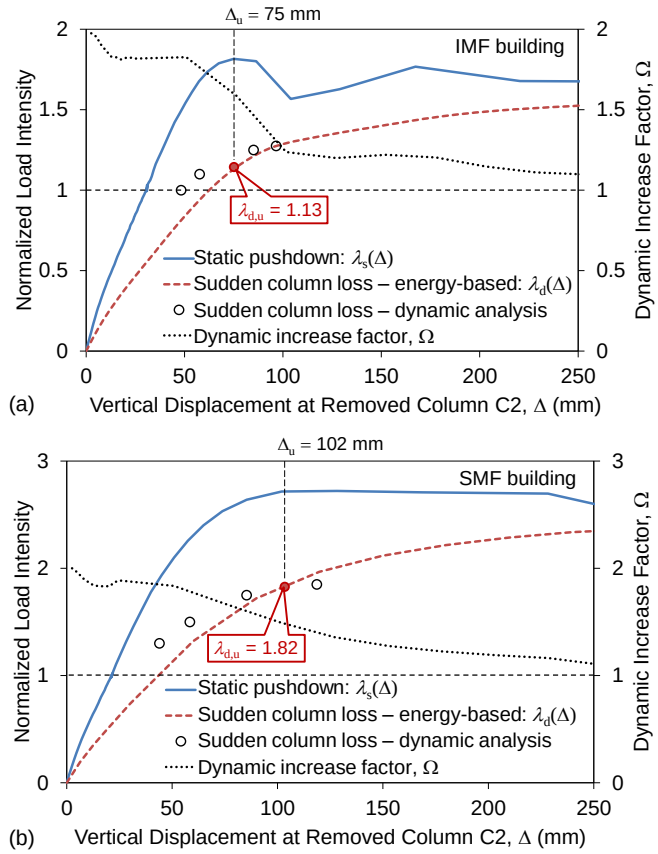

Fig. 15. Analysis results for prototype buildings under loss of column C2: (a) IMF building; (b) SMF building

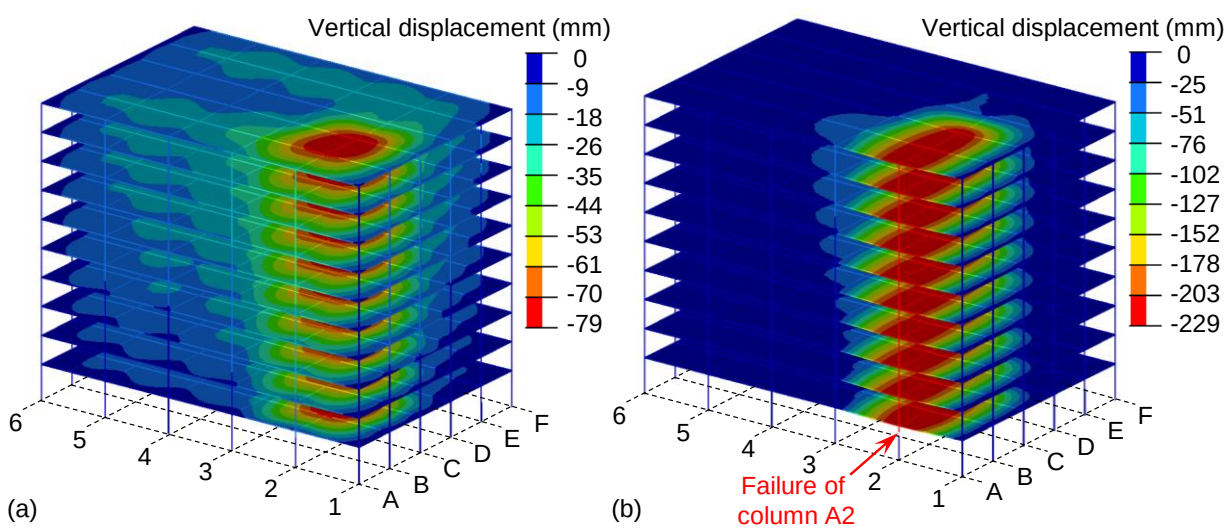

Fig. 16. Vertical displacement contours from static pushdown analysis of IMF building with column C2 removed: (a) Δ = 75 mm; (b) Δ = 220 mm